Available online at www.sciencedirect.com
ScienceDirect
Advances in Space Research 42 (2008) 403–408
ADVANCES IN SPACE RESEARCH (a COSPAR publication)
www.elsevier.com/locate/asr

First measurements of cosmic-ray nuclei at high energy with CREAM

S.P. Wakely [a,*], H.S. Ahn [b], P. Allison [d], M.G. Bagliesi [e], J.J. Beatty [d], G. Bigongiari [e], P. Boyle [a], T.J. Brandt [d], J.T. Childers [f], N.B. Conklin [g], S. Coutu [g], M.A. DuVernois [f], O. Ganel [b], J.H. Han [h], J.A. Jeon [h], K.C. Kim [b], M.H. Lee [b], L. Lutz [b], P. Maestro [e], A. Malinine [b], P.S. Marrocchesi [e], S. Minnick [i], S.I. Mognet [g], S.W. Nam [h], S. Nutter [j], I.H. Park [h], J.H. Park [h], N.H. Park [h], E.S. Seo [b,c], R. Sina [b], S.P. Swordy [a], J. Wu [b], J. Yang [h], Y.S. Yoon [b], R. Zei [e], S.Y. Zinn [b]

[a] *Enrico Fermi Institute and Department of Physics, University of Chicago, Chicago, IL 60637, USA*
[b] *Institute for Science and Technology, University of Maryland, College Park, MD 20742, USA*
[c] *Department of Physics, University of Maryland, College Park, MD 20742, USA*
[d] *Department of Physics, Ohio State University, Columbus, OH 43210, USA*
[e] *Department of Physics, University of Siena and INFN, Via Roma 56, 53100 Siena, Italy*
[f] *School of Physics and Astronomy, University of Minnesota, Minneapolis, MN 55455, USA*
[g] *Department of Physics, Penn State University, University Park, PA 16802, USA*
[h] *Department of Physics, Ewha Womans University, Seoul 120-750, Republic of Korea*
[i] *Department of Physics, Kent State University, Tuscarawas, New Philadelphia, OH 44663, USA*
[j] *Department of Physics and Geology, Northern Kentucky University, Highland Heights, KY 41099, USA*

Received 31 October 2006; received in revised form 5 January 2007; accepted 22 March 2007

Abstract

The balloon-borne cosmic-ray experiment CREAM-I (Cosmic-Ray Energetics And Mass) recently completed a successful 42-day flight during the 2004–2005 NASA/NSF/NSBF Antarctic expedition. CREAM-I combines an imaging calorimeter with charge detectors and a precision transition radiation detector (TRD). The TRD component of CREAM-I is targeted at measuring the energy of cosmic-ray particles with charges greater than $Z \sim 3$. A central science goal of this effort is the determination of the ratio of secondary to primary nuclei at high energy. This measurement is crucial for the reconstruction of the propagation history of cosmic rays, and consequently for the determination of their source spectra. First scientific results from this instrument are presented

PACS: 95.85.Ry; 95.55Vj; 96.50.Sb; 29.40.Cs; 29.40.Ka; 29.40.Mc

Keywords: Cosmic rays; Energy spectrum; Charge; TRD; Cerenkov detector

1. Introduction

The Cosmic-Ray Energetics and Mass (CREAM) instrument is a balloon-borne instrument designed to make direct measurements of the energy and elemental composition of cosmic rays at high energies. The first flight of this instrument took place during the 2004–2005 NASA/NSF/NSBF Antarctic balloon campaign and was successfully completed in January of 2005, after 42 days afloat (see Seo et al., 2005).

The CREAM payload comprises a suite of complementary instruments, including charge and velocity detectors, a gas transition radiation detector (TRD), and a thin Tungsten/scintillating-fiber sampling calorimeter. The inclusion of multiple instruments allows for cross-calibration and

* Corresponding author.
E-mail address: wakely@uchicago.edu (S.P. Wakely).

0273-1177/$34.00 © 2007 COSPAR. Published by Elsevier Ltd. All rights reserved.
doi:10.1016/j.asr.2007.03.080

reduction of systematic errors. Here we discuss results obtained using the "Hi-Z" subset of detectors, which is specifically designed to measure particles with nuclear charge $Z \gtrsim 3$. This detector set includes the TRD, the Cerenkov velocity detector and the timing charge detector.

2. Science goals

One of the primary scientific goals of the CREAM project is the measurement of secondary cosmic-ray nuclei at high energies. Secondary nuclei are those nuclei which are produced predominantly through spallation interactions of primary nuclei (*i.e.*, those which are produced in the cosmic-ray source regions). Because these spallation interactions are thought to occur primarily during the propagation of primary nuclei in the interstellar medium, a measurement of the ratio of secondary/primary fluxes reveals information about the propagation history (*e.g.*, the amount of material traversed) of the primary particles.

Previous measurements have shown (see, *e.g.*, Swordy et al., 1990 and Engelmann et al., 1990 and references therein), somewhat surprisingly, that this ratio is not constant with energy. Instead, it appears to drop in a manner which is consistent with a simple power-law rigidity-dependent (*i.e.*, $\propto R^{-\delta}$) model of escape from the Galaxy (Swordy, 2001). This results in a modification of the cosmic-ray energy spectrum, such that the power-law spectral index is flatter at the particle source by the value δ. Current data on the ratio of Boron to Carbon (B/C) extend up to ~200 GeV/nuc, and appear to favor $\delta \sim 0.6$, which, when combined with the observed index of the overall energy spectrum (~2.7), matches well to the predicted source spectra from diffusive shock acceleration models (~2.0, see Bell, 1978a,b; Blandford and Ostriker, 1978; Krymsky, 1977). Similar results for δ are obtained from the study of the so-called sub-Fe ($Z = 21$–24) to Fe ratio (*e.g.*, Engelmann et al., 1990).

Extending these measurements to higher energies, with improved statistics, is one of the goals of CREAM, and will help determine whether the ratio continues to drop, or whether it approaches some constant value at high energies, which is probably required to match anisotropy measurements (Swordy, 1993). Crucial to this goal is a large instrument with excellent charge resolution. Size is needed to capture sufficient high energy particles, and charge resolution is needed to efficiently identify primary particles, which, with fluctuations, can contaminate the much smaller secondary sample (B/C at ~200 GeV/nuc is ~5%).

3. Instrument design

The CREAM instrument combines several individual detector systems, including a timing charge detector (TCD), a transition radiation detector, a plastic Cerenkov detector, a pixelated silicon charge detector (SCD), and an imaging thin calorimeter (CAL). The combination of redundant and complementary detection systems (*i.e.*, TCD/SCD and TRD/CAL) allows for cross-calibration and the reduction of systematic errors. A detailed description of all the CREAM components can be found in Seo et al., 2002; here we review only the design of the Hi-Z system: the TCD, the TRD and the Cerenkov detector. A schematic view of this instrumentation is shown in Fig. 1.

3.1. Timing charge detector

The TCD system includes 8 scintillator paddles arranged into orthogonal X & Y layers. The paddles are 1.2 m-long, 5 mm-thick slabs of Bicron BC-408 read out with Photonis XP2020UR fast timing photomultiplier tubes (PMTs) through twisted-strip BC-802 adiabatic light guides. The light guides are doped with UV absorber, which reduces Cerenkov production in the guides without impacting the scintillation signal. Each paddle is viewed on both ends by a photomultiplier tube. The signals from the TCD, in conjunction with the Cerenkov detector, are used to generate the instrument's Hi-Z trigger, and (again jointly) to measure the charge of incoming particles.

The detector has been designed to provide the charge resolution needed to easily resolve individual elements over the entire relevant charge range (*e.g.*, ~0.2e for Oxygen and ~0.35e for Iron). For improved dynamic range, the amplitude of each PMT signal is measured at four different dynodes and fed into independent electronics channels. The timing structure of each pulse's leading edge is also captured – with 50 ps accuracy – in each channel of electronics. This fast timing information helps in rejecting possible albedo particles produced by interactions of primary particles with the calorimeter. These particles arrive 3–8 ns after the initial passage of the primary particle. Fast timing can also aid in the discrimination between light

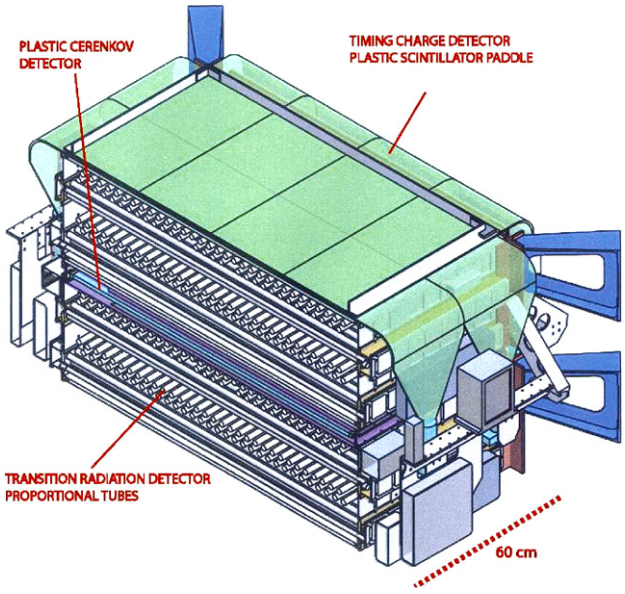

Fig. 1. A schematic cross-sectional view through the middle of the CREAM Hi-Z detector systems. Shown are the Timing Charge Detector (TCD), Transition Radiation Detector (TRD) and Cerenkov Detector systems.

nuclei species, as the risetime of pulses from low-Z nuclei has a measurable dependence on Z (Beatty et al., 2003).

3.2. Transition radiation detector

The CREAM TRD is constructed of 512 thin-walled gas proportional tubes filled with a mixture of 95% Xenon/5% Methane at 1 atm. The 2 cm-diameter tubes are 1.2 m-long and are wound from thin (100 μm) mylar to allow easy penetration by the relatively low-energy transition radiation X-rays. The tubes are fixed in a matrix of polystyrene foam radiator and arranged in 8 layers of 64 tubes, with alternating orthogonal X and Y orientations. The tubes themselves are mounted at each end with an O-ring seal into gas manifolds. The manifold at one end also contains electronics boards for high voltage distribution and signal collection from the sense wires, which are held at positive high voltage in the range of 1–2 kV. The signals from each tube are read out with a simple dual-gain system utilizing two channels of an Amplex 1.5 ASIC, achieving better than 11-bit overall effective dynamic range.

The TRD is designed to provide a measurement of the Lorentz factor of the primary particle as it traverses the detector, and hence it is configured as a precision TRD (see, *e.g.*, Wakely, 2002), rather than a threshold TRD. Additionally, the TRD can provide particle tracking, producing a 3D particle trajectory which, using the simplest linear reconstruction methods, can achieve an RMS position resolution of $\sigma \sim 5$ mm. Accurate trajectory information is crucial for applying proper response map corrections to the TCD and Cerenkov systems.

3.3. Cerenkov detector

The CREAM Cerenkov detector consists of a 1 cm-thick 1.2 m × 1.2 m acrylic sheet doped with blue wavelength shifter. This radiator is surrounded by 4 bars of wavelength-shifting plastic butted against the 4 edges of the sheet. These bars shift the blue radiator photons into the green wavelength range, where they are read out with 2 photomultipliers, one at each end of the bars. This design provides a compact detector with a relatively uniform response.

The Cerenkov threshold of the radiator material is roughly $\gamma \sim 1.35$ and the participation of the Cerenkov detector in the instrument trigger enables the rejection of the many low-energy particles in the cosmic-ray flux at high latitudes. The signals in this detector also provide information complementary to the TCD on the charge of the incident primary particles. Because the Cerenkov detector is not segmented, a signal contribution from delta-rays generated in upstream material must be accounted for in the response function. This effect is understood and can be modeled with detailed simulations.

Without any mapping corrections, the Cerenkov response is uniform to within roughly 20% across the face of the detector. However, flight data can be used to generate a correction map, which improves the flatness in response significantly. Fig. 2 shows the response of the Cerenkov detector to incident Oxygen nuclei, after the application of mapping corrections. These corrections flatten the detector response to within roughly 2% over ~95% of the detector area.

4. Flight and instrument performance

The CREAM payload was launched from McMurdo on 16 December, 2004, and successfully circumnavigated the South Pole three times during its record-breaking 42-day flight. The average altitude throughout the flight was ~128,000 ft, corresponding to an overburden of only ~3.9 g/cm^2. During this time, roughly 40 million Hi-Z triggers were collected and written to disk.

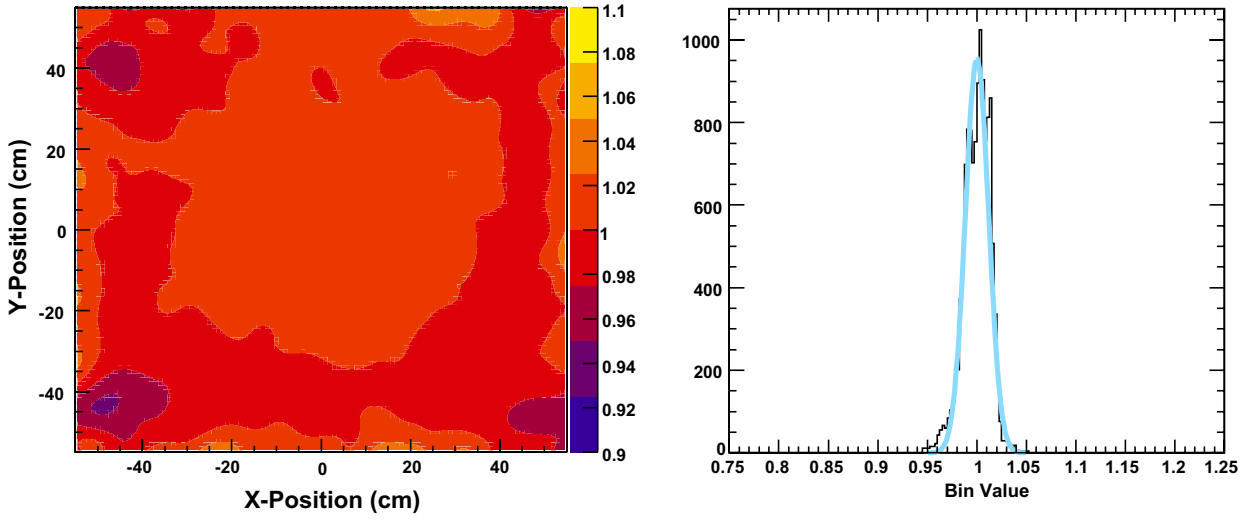

Fig. 2. Cerenkov response map for Oxygen nuclei, after mapping corrections. The left panel shows a contour plot showing the normalized response of the Cerenkov detector to incident Oxygen nuclei. The right panel shows a histogram of the bins on the contour plot, showing roughly 95% of all bins within 2% of the overall mean.

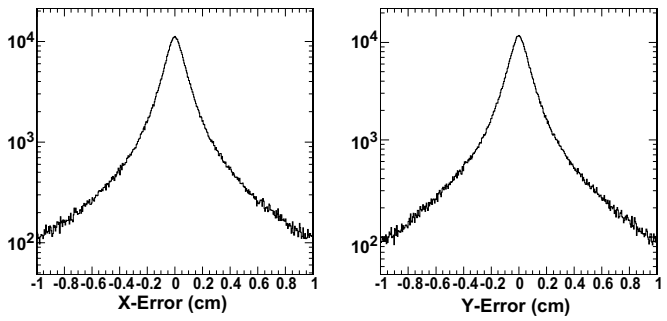

Fig. 3. Simulated TRD tracking error for incident Oxygen nuclei. The left pane shows the reconstruction error in x direction. The right pane shows the reconstruction error in the y direction. In both panes, note the ordinate scale is logarithmic.

Despite operating without a pressure vessel in a near vacuum of a few mbar, all of the detector systems performed well throughout the flight. In particular, the loss rate in the gas system of the TRD was very low, amounting to only ~10% of the system (not reserve) volume over the entire flight. Though it comprises nearly 600 m of thin-walled tubing, the TRD's leak rate was low enough that no "make-up" gas was required throughout the flight. Instead, a periodic redistribution of gas between manifolds was performed; this proved sufficient for maintaining good detector response from all layers throughout the flight. Also of note was the stability of the signal response over the course of the flight. Despite having no fresh gas provided throughout the flight, the tube resolution did not noticeably degrade. This is unusual, as similar systems operated with overpressure at ground-level typically lose resolution over timescales of 1/2 day or so, suggesting that diffusion of ambient electronegative oxygen into the chambers is the most likely cause of signal resolution loss. The loss rate at altitude is at least 100 times lower. This performance demonstrates that this general TRD design is well-suited for a future long duration balloon or space-based mission.

All of the other systems performed quite well throughout the flight, though one of the eighteen TCD photomultiplier tubes failed near the end of the flight. The instrument was even able to recover and continue collecting data after being struck on 20 January, 2006 by one of the most intense solar flares ever observed (Yoon et al., 2005; Mewaldt et al., 2005).

4.1. TRD tracking and signal resolution

Monte Carlo simulations indicate that with very simple linear fitting algorithms, the TRD can provide an RMS tracking resolution of $\sigma \sim 5$ mm. A second-level likelihood fit which takes the tube geometry and impact parameters into consideration can improve this to better than 2 mm. This is demonstrated in Fig. 3, which shows the results of a Monte Carlo test of the tracking accuracy. The performance demonstrated in Monte Carlo was verified with flight data by selecting particle trajectories which scan across gaps between the 30 cm TCD paddles and looking for the deficits in the TCD signals due to corner-clipping.

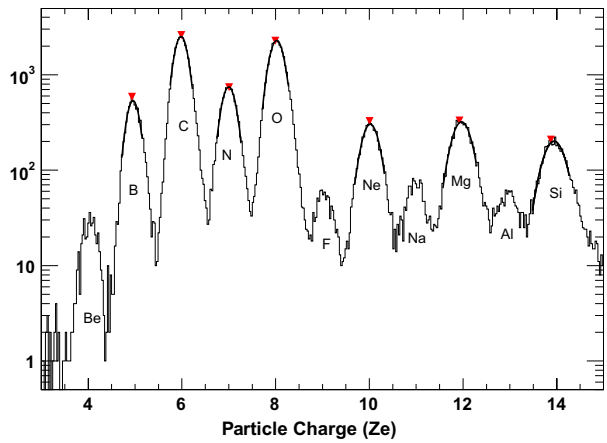

Fig. 4. Preliminary charge spectrum (for all energies) produced by using a combination of TCD and Cerenkov detector signals. Well separated charge peaks are visible for all elements from Beryllium to Silicon. The lines indicate Gaussian fits to the more prominent peaks.

Another important component of the TRD tracking system is the precision with which energy loss per unit pathlength over the entire track can be determined. This resolution has a direct impact on the ultimate energy resolution achievable with the instrument, and must be sufficiently good to achieve the science goals of the mission. Furthermore, a detailed knowledge of how this resolution changes with energy is required to properly deconvolve measured energy spectra. By using the X and Y projections of the TRD tubes as independent detectors, however, we are able to test this resolution and compare it to Monte Carlo simulations. Such an analysis suggests the dE/dx resolution for through-going Oxygen nuclei is an acceptable ~7%.

4.2. Charge resolution

For an accurate determination of the primary to secondary cosmic-ray ratio, a good separation between the adja-

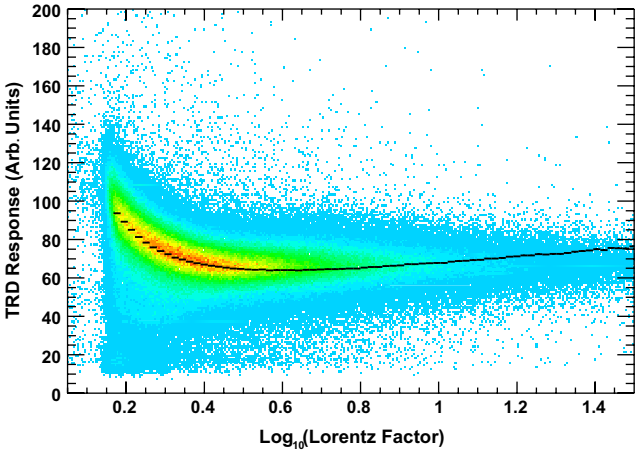

Fig. 5. Comparison of the TRD energy deposit vs Log_{10}(Lorentz Factor) for simulated and measured Oxygen nuclei. The flight data are shown in the scatter plot and the mean of the simulation results is shown with the black line. The deviation at higher γ is expected, as the Cerenkov yield saturates. For the real data, γ is calculated by combining Cerenkov and TCD data.

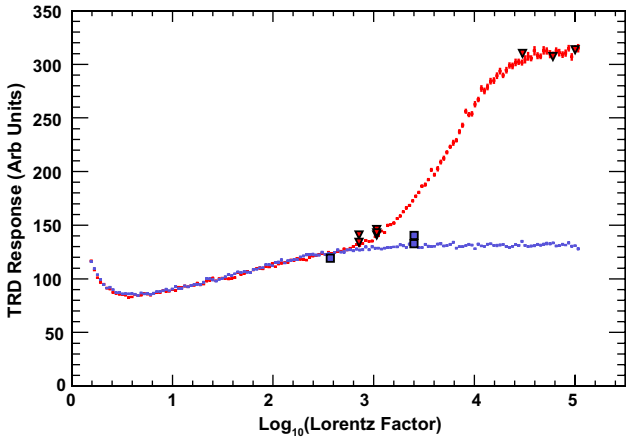

Fig. 6. GEANT4 simulations of gas detector response. The lines show the simulation response with (red) and without (blue) a transition radiator present. The red triangles and blue squares show the response measured in a beam-test at CERN with and without a radiator.

cent charges (*e.g.*, B and C) is very important. Fig. 4 shows a preliminary charge spectrum for lower-Z ($Z < 15$) nuclei, as measured in CREAM. This figure was produced by combining the signals from the Cerenkov detector and the TCD to produce a velocity-independent charge estimate. Mapping corrections and additional corrections for gain drift, electronics non-linearity and signal attenuation have been applied. The resultant resolution exceeds the design goals of the TCD, approaching an RMS width of ~2% for Oxygen nuclei.

4.3. Energy calibration

The energy of incident primary nuclei can be determined by examining the rate of ionization energy deposit in the TRD system. At energies below ~1 TeV/nucleon, the determination relies on the logarithmically-increasing "relativistic rise" of ionization energy loss, which is relatively large in Xenon (plateau/MIP ~ 1.5). Above this energy, the additional contribution from X-ray transition radiation photons improves the measurement, up to Lorentz factors of $\gamma \sim 20000$.

In both cases, however, it is important to calibrate the detector response with test beam data and Monte Carlo simulations. For instance, Fig. 5 shows the response of the CREAM TRD versus Lorentz factor (γ) for incident Oxygen nuclei (contour plot), overlaid with the mean response predicted by a full GEANT 4.7.1p01 (Geant4 Collaboration, 2003) detector simulation (black line). For flight data, the Lorentz factor is calculated using the combined response of the Cerenkov and TCD detectors. The well-matched response near ionization minimum indicates that we understand and can properly simulate the detector response and therefore have a reasonable energy calibration at low energy. The deviation between data and Monte Carlo at higher Lorentz factor is fully expected, as the Cerenkov emission yield saturates beyond $\gamma \sim 10$.

With a minor modification to the code (which simply doubles the number of transition radiation photons produced) the GEANT4 simulation package also appears to properly reproduce the production of transition radiation at higher Lorentz factors. Fig. 6 shows a comparison of Monte Carlo results to data collected in a beam-line test in 2001 at CERN (Swordy et al., 2003). Here, the red and blue lines show, respectively, the simulated gas detector response with and without a transition radiator volume inserted in the beam-line. The rise in the red line above $\log_{10}(\gamma) \sim 3$ is due to the onset of transition radiation production. On this plot, the red triangles and blue squares indicate measurements made during the beam-test with and without a radiator volume present. These tests confirm that our energy calibration at high energy is also adequate.

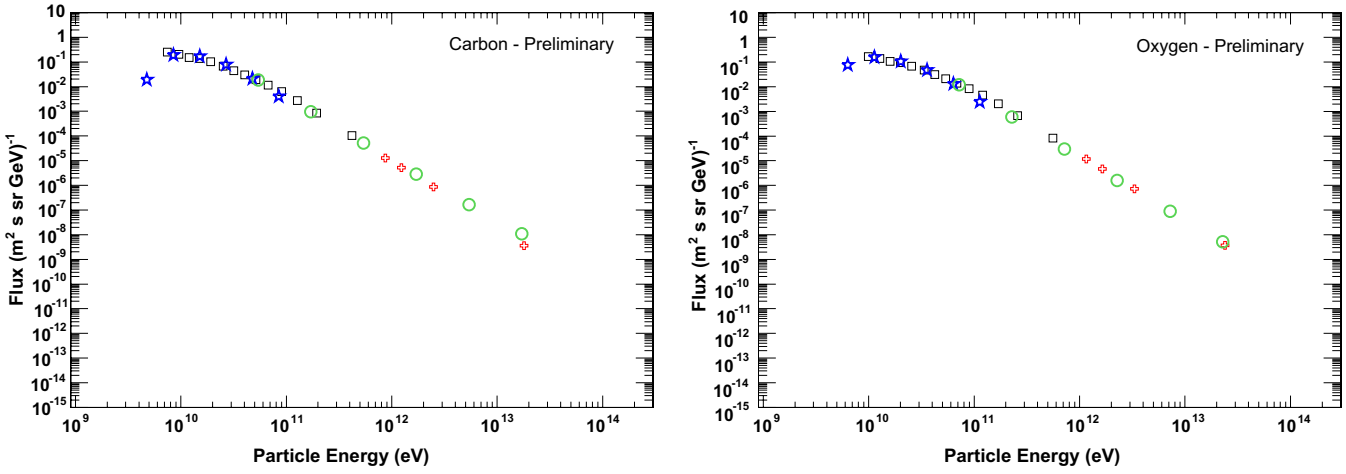

Fig. 7. Preliminary cosmic ray energy spectra, measured with the CREAM Hi-Z system. The left panel shows the spectrum for cosmic Carbon nuclei; the right panel shows the spectrum for Oxygen nuclei. In both panels, the black squares represent data collected by the HEAO experiment (Engelmann et al., 1990), and the red crosses are from the CRN experiment (Swordy et al., 1993). The blue stars and green circles represent events with energies reconstructed by the CREAM Cerenkov and TRD detectors, respectively. The normalization of the CREAM points have been adjusted with a single overall parameter applied in both panels and both detector results.

5. Results and discussion

After calibrating the detector response curves, as discussed above, the measured energy deposit in the Hi-Z detector systems can be used to reconstruct the energy of the incident cosmic-ray events. Fig. 7 shows the preliminary results of this procedure for Carbon and Oxygen nuclei. In these figures, the energy as reconstructed using the Cerenkov determination of β is indicated with blue stars, while the energy as determined using the relativistic rise in the TRD gas detectors is indicated with the green circles. Overlap corrections which account for the finite energy resolution of the detectors have been applied and the bin sizes have been selected to be $\sim 1.5\sigma$ wide in energy resolution. As shown, the two differing techniques show good agreement where they overlap ($\sim 10^{11}$ eV).

Also shown on the plots are the results of two space-based missions, the HEAO experiment (black squares – Engelmann et al., 1990) and the CRN experiment (red crosses – Swordy et al., 1993). The CREAM results have been arbitrarily normalized (with a single normalization constant across all four measurements) to match the HEAO flux at around ~4 GeV/nuc. Still, the overall agreement between the three experiments is rather good. The results for the Oxygen spectrum also agree with recent results from the TRACER instrument (Boyle, 2005). Remarkably, the CREAM results span over three orders of magnitude.

Though the results presented in Fig. 7 extend only up to ~1 TeV/nuc, the total exposure factor of the CREAM-I flight (~30 m^2 sr days after initial cuts) was sufficient to collect abundant primary nuclei (*e.g.*, C & O) up to energies nearly twenty times higher than this. However, as can be seen on Fig. 6, the energy range above ~1 TeV/nuc (Lorentz factor ~1000) corresponds to the region where the TRD detector response is dominated by the contributions of transition radiation processes. As a result of this shift, the TRD response and signal resolution in this region must be very well understood in order to properly deconvolve the measured spectra. Cross calibration from the CREAM calorimeter should help in this regard, and this work is underway. Once completed, we expect measurements of Oxygen nuclei to extend up to $\sim 3 \times 10^{14}$ eV total energy, and anticipate extending current measurement of the B/C ratio to ~500 GeV/nuc.

6. Conclusions

The first results of the Hi-Z system of the CREAM-I instrument have been presented. After a 42-day flight during which the whole detector operated stably and efficiently, a preliminary analysis of the data indicates that the individual detectors performed very well. Furthermore, the response of the Hi-Z system appears to match the Monte Carlo simulations, and hence the response of the detectors can be well calibrated, although additional work is underway to guarantee all systematic effects are accounted for. Following this work, results on the fluxes of cosmic nuclei from Boron to Iron, over three decades in energy will be presented.

Acknowledgements

This work was supported in the United States by NASA, by INFN and PNRA in Italy and by the MOST/KOSEF Creative Research Initiative in South Korea. The authors appreciate and acknowledge the support of NASA/WFF, the CSBF, and the NSF Office of Polar Programs.

References

Beatty, J.J., Ahn, H.S., Allison, P.S., et al. The cosmic ray energetics and mass (CREAM) experiment timing charge detector, in: Gorham, P.W. (Ed.), Particle Astrophysics Instrumentation. Proceedings of the SPIE, vol. 4858, pp. 248–254, 2003.

Bell, A.R. MNRAS 182, 147, 1978a.

Bell, A.R. MNRAS 182, 443, 1978b.

Blandford, R.D., Ostriker, J.P. ApJ Lett. 221, L29, 1978.

Boyle, P.J., Ave, M., Gahbauer, F., et al. Energy spectra of heavy cosmic ray nuclei from 0.5 GeV/amu to 10,000 GeV/amu, in: International Cosmic Ray Conference, pp. 65–68, 2005.

Engelmann, J.J., Ferrando, P., Soutoul, A., et al. Charge composition and energy spectra of cosmic-ray nuclei for elements from Be to NI – Results from HEAO-3-C2. Astron. Astrophys. 233, 96–111, 1990.

Geant4 Collaboration. Geant4-a simulation toolkit. Nucl. Instrum. Methods Phys. Res. A, 506, 250–303, 2003.

Krymsky, G.F. Dokl. Akad. Nauk. USSR 236, 1306, 1977.

Mewaldt, R.A., Cohen, C.M., Leske, R., et al. Solar Energetic Particle Composition, Energy Spectra and Timing in the January 20, 2005 Event. AGU Fall Meeting Abstracts, A320, 2005.

Seo, E.S., Ahn, H.S., Beach, S., et al. Cosmic-ray energetics and mass (CREAM) balloon experiment. Adv. Space Res. 30, 1263–1272, 2002.

Seo, E.S., Ahn, H., Allison, P., et al., The record breaking 42-day balloon flight of CREAM, in: International Cosmic Ray Conference, pp. 101–105, 2005.

Swordy, S., in: Proceedings of the 23rd International Cosmic Ray Conference, pp. 243–246, 1993.

Swordy, S.P. The energy spectra and anisotropies of cosmic rays. Space Science Reviews 99, 85–94, 2001.

Swordy, S.P., Boyle, P., Wakely, S. Comparison of a transition radiation detector response with numerical simulations, in: International Cosmic Ray Conference. pp. 2233–2236, 2003.

Swordy, S.P., L'Heureux, J., Meyer, P., Muller, D. Elemental abundances in the local cosmic rays at high energies. Astrophys. J. 403, 658–662, 1993.

Swordy, S.P., Mueller, D., Meyer, P., et al. Relative abundances of secondary and primary cosmic rays at high energies. Astrophys. J. 349, 625–633, 1990.

Wakely, S.P. Precision X-ray transition radiation detection. Astroparticle Phys. 18, 67–87, 2002.

Yoon, Y., Ahn, H.S., Allison, P., et al. CREAM Observation of January 20th Solar Flare. AGU Fall Meeting Abstracts, A314, 2005.